Fault Analysis of Electrical Machine Drives Employing

Novel Model Predictive Control

Yogita P. Akhare, Warsame H. Ali, John H. Fuller and John O. Attia

Roy G. Perry College of Engineering

Prairie View A&M University

Prairie View, Texas

USA

_____

ABSTRACT

Electrical machine drives play a crucial role in various industrial applications. Therefore, its control system design became more significant in the last decades. Numerous high powers and high-efficiency machine drives require faultless continuous operation. Fault-tolerant control is a productive solution for the improvement of the reliability of the machine drives. Model Predictive Control (MPC) is an optimal control algorithm developed for constrained control of Multi-Input-Multi-Output (MIMO) systems. MPC can handle MIMO systems and can incorporate several constraints in the form of equalities and inequalities. A Novel Model Predictive Control (NMPC) method for a Synchronous Servo Motor Drive (SSMD) integrating a real-time fault diagnostic method for Insulated Gate Bipolar Transistor ((IGBT) faults in an inverter have been presented in this paper. NMPC ensures the system's better performance and minimal fault clearance time.

Key Words: Novel Model Predictive Control (NMPC), MPC, Synchronous Servo Motor Drive (SSMD), Insulated-Gate Bipolar Transistor (IGBT).
_____

1. INTRODUCTION

Nowadays, Servo drives are used for numerous production facilities and are employed where the dynamic, automatic variable speed drives are necessary. Servo drives consist of a permanent-magnet synchronous motor (PMSM) provide with an inverter unit [1]. Synchronous servo motor drives (SSMD) are extensively used in the control system to turn the electrical signal to a motor's mechanical displacement [2]. A variable frequency inverter in controlled speed synchronous motor drives provides synchronous speed to overcome the fixed speed limitation resulting from the mains constant frequency [3]. Among all the faults of synchronous servo drives, a single-phase open circuit (SOCF) fault as usual, in which one phase winding disconnected from the VSI [4]. The performance of the motor does not remain valid under short circuit fault condition. For this cause, some researchers have studied their proposed model using MATLAB /Simulink and validated experimentally to detect the effects of faults in an electrical machine [5-7]. Various control methods proposed for multiphase machines with open-circuit faults [8]. For predicting the system's future behavior and cost function minimization, MPC is presented [9]. Researchers proposed many advanced current control strategies such as Predictive current control [10-17], Hysteresis control [18], and Fuzzy PI control [19] to find the rapid response of the current control loop. PCC method tracks the current reference rapidly and accurately by taking both stability and small current harmonic components into account [20]. PID controllers have easy structure and few parameters that operators could change to improve the controller's performance. PID controllers do not provide optimal control inputs [21]. A more advanced control approach is a Linear Quadratic Regulator (LQR), which offers optimality. LQR solves an optimization problem of minimization of the state and inputs over the infinity prediction horizon subject to a linear constraint, which is the system's linear model. LQR cannot handle other constraints, but it applies to MIMO systems without decoupling [22]. Two different MPCs needed for routine and post fault operations of PMSM drives as a model-based control, making the whole control method complicated [23-26]. To a certain extent, MPC faces a problem in achieving the robustness against model mismatches and noises [27-30]. Modern MPC algorithms can perform some specific features such as more constraints [31-33], reduction in online computation [34]. However, there is a concern to find a computationally, reliable, and efficient MPC algorithm [35].

A novel model predictive controller (NMPC) is designed for synchronous servo motor drive (SSMD) considering single-phase open-circuit fault (SOCF), short circuit fault (SCF), and demagnetization fault (DF). First, the mathematical modeling of SSMD for the pre-fault and post-fault operation has been introduced, followed by the advancement of the NMPC. The NMPC then employs for the prediction of current in a discrete-time calculation. The phase current can be estimated at the next sampling step to compensate for the current errors, with the modification of three-phase currents of the motor. The machine's speed responses using traditional control methods compared with the NMPC under different load and speed references for various fault conditions. The experiments conducted on the Lucas Nulle servo drive system for all the faults occur in machine drive to validate the simulation results. The complete analysis and the simulation and experimental results show that with the adoption of NMPC, fault clearance time for all the different types of faults occurs in the servo drive system is intensively low compared to the conventional controllers.

2. MODEL PREDICTIVE CONTROL

2.1 Recent control and modulation schemes for industrial drive

Control and modulation schemes for industrial drives used recently are listed below:

- **Direct Torque Control (DTC):**
  Analysis of PMSM shows that electromagnetic torque is proportional to the angle between the stator and rotor flux linkages. The stator flux linkage's rotating speed needs to increase for the direct torque control method's fast torque response. Compared to vector control methods, the direct torque control has a simple structure that allows the easy implementation to the digital signal controller. Also, DTC has high robustness and minimal torque response time due to which a high dynamic performance of the drive can be achieved [36-37].
- **Direct Power Control (DPC):**
  In this method, active and reactive powers are regulated in a fixed switching frequency with a space vector modulation (SVM) technique. DPC-SVM has a unique feature in active and reactive power with a continuous switching frequency and low ripples [38].
- **Field-Oriented Control (FOC):**
  In this scheme, an orthogonal current vector component controls the position of a servo motor. The stator currents are considered two different vectors: the torque and the motor's magnetic flux [39].
- **Voltage-Oriented Control (VOC):**
  VOC has a cascaded control structure with an outer dc-link voltage control loop and an inner current control loop. A minimum dc-link voltage is necessary to obtain undistorted current waveforms for the proper operation of the rectifier. All the six diodes need to be polarized negatively at all the ac-voltage supply values for the rectifier's full control [40].
- **Carrier-Based Pulse Width Modulation (CB-PWM):**
  CB-PWM is the modulation process used in most communication systems to encode a signal's amplitude into a pulse width, usually a carrier signal, for transmission [41].
- **Space Vector-Pulse Width Modulation (SV-PWM):**
  SV-PWM is the final step in the field-oriented control technique to generate the motor's desired three-phase voltages. In this technique, a steady-state DC-voltage is provided to the inverter's six switches to create a frequency and amplitude adjustable sinusoidal waveform [42].
- **Volts Per Frequency (V/f) Control with Optimized Pulse Patterns (OPPs):**
  MV converter systems mostly use OPPs. Optimized pulse patterns (OPPs) allow minimizing the current distortions for a given switching frequency [43].
- **Model Predictive Control (MPC):**
  MPC is an advanced control technique that controls the multi-input multi-output (MIMO) process satisfying inequality constraints impacted by the input and output variables. Model and current measurements predict the outputs' future values if a feasible and accurate dynamic model of the process is available. The predictions and measurements are used for calculation of the appropriate changes in the input variables [44].

2.2 Comparison of MPC with other control methods

Figure 1. shows the comparison of MPC with other control methods. MPC combines the advantages of DTC or DPC during transients with the benefits of offline computed OPPs during steady-state operation. The bandwidth (response time for changing input command) is fast for MPC, and it has very low distortion and switching losses.
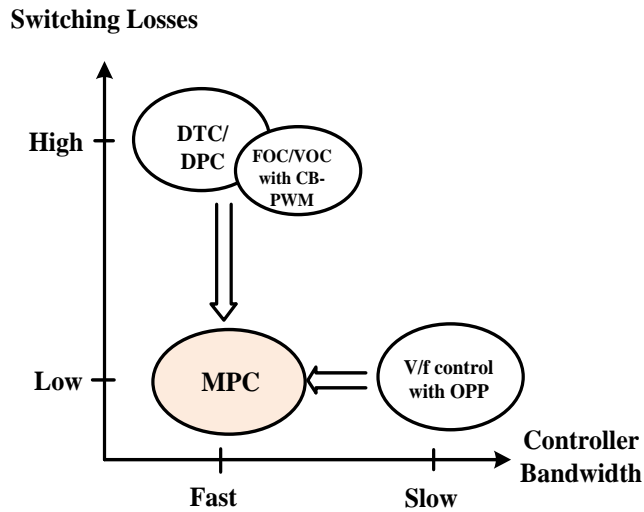
Figure 1. Comparison of MPC with other control methods [45]

2.3 Fundamental Structure of MPC

The objective of an MPC is to prevent violations of input and output constraints. It drives some output variables to their optimal set points while maintaining other outputs within specified ranges. In addition to this, it prevents excessive movement of the input variables. MPC can control as many process variables as possible when a sensor or actuator is not available. MPC's main objective is to maximize a profit function while minimizing a cost function or maximizing a production rate [46]. Figure 2 shows the fundamental structure of the MPC.
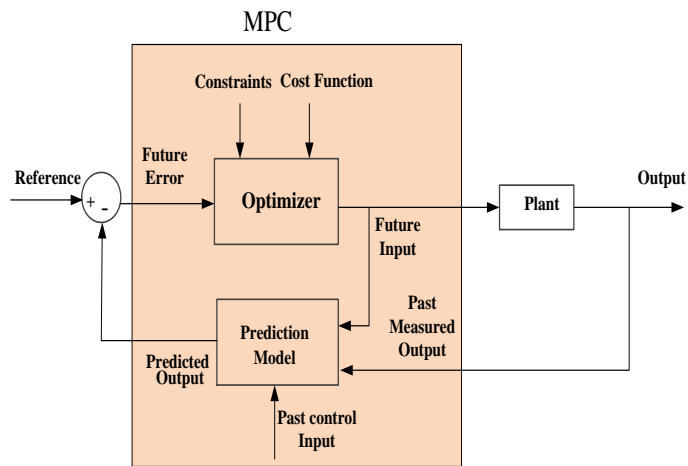

Figure 2. Fundamental Structure of the MPC.

2.4 Working Principle of MPC

The future outputs are predicted at each sampling instant t considering the dynamic output of the plant for the prediction horizon N. These predicted outputs y (t+ k) depends on the known values up to instant t (past inputs and outputs) and the future control signals u (t + k). A model is used to predict future plant outputs based on past and current values and the proposed optimal future control actions [47]. The optimizer's actions are calculated considering the cost function and the constraints, as shown in Figure 3.
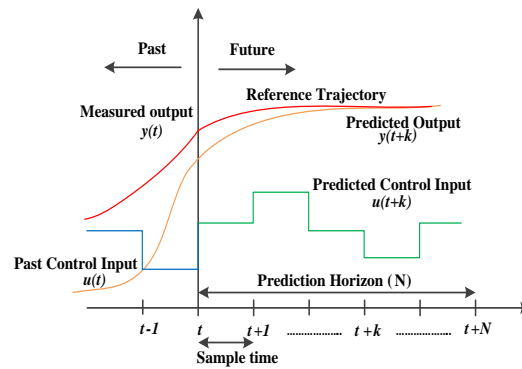
Figure 3. Working Principle of the MPC.

The economic optimization based on a steady-state model of the process calculates the control action' set points. The current measurements and predictions of the future values of the outputs determine the MPC calculations are based. The MPC control calculations' objective is to select a sequence of control moves (manipulated input changes) so that the predicted response optimally moves to the set-point [48]-[49].

3. FAULT-TOLERANT CONTROL AND DYNAMIC MODELLING FOR NMPC

3.1 Fault-Tolerant Control of PMSM Drive

Figure 4 shows the fault-tolerant control analogy. The PMSM neutral point N connected to the mid-point of the DC bus capacitor link. This analogy mitigates both open circuits as well as short circuit fault. It comprises a conventional three-phase drive and three fast-acting fuses connected in series with the stator windings. A triac TR_n is used for the control of open circuit fault and triacs TR_a, TR_b and TR_c are used for the short circuit fault. The triacs remains OFF during the normal operating condition of the drive. When a fault occurs, the faulty leg will be isolated first, and then the triac will be turned ON. Triacs turned OFF during the normal operating condition of the drive. When a fault occurs, the faulty leg will be isolated first, and then the triac will be turned ON. The neutral point is needed to control the currents' amplitude and phase in the remaining two healthy phases. The currents in the remaining two healthy phases should be regulated to a magnitude of $\sqrt{3}$ times their original value, and phase-shifted 60^0 with respect to each other to maintain the torque and the motor's performance.
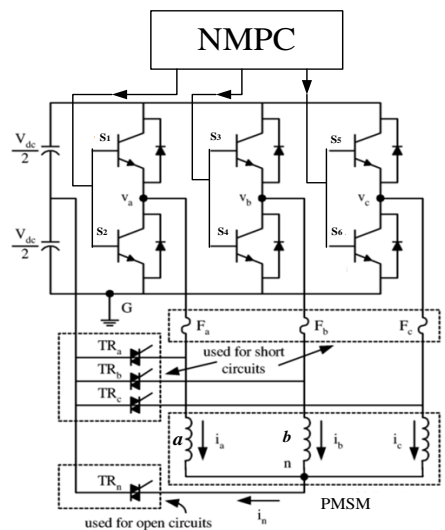

Figure 4. Fault-tolerant drive with neutral point connected to the middle of the
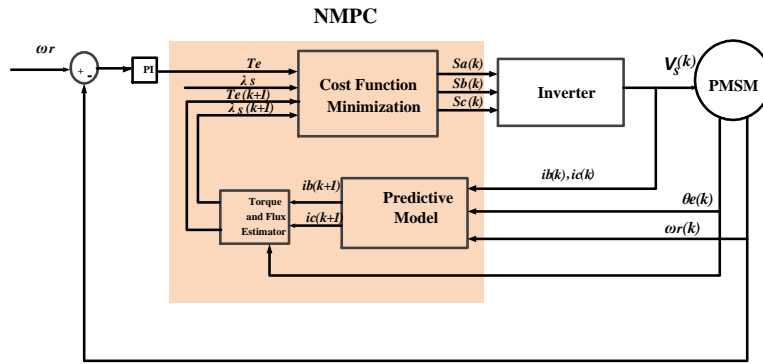**VSI DC-link**

Figure 5. Control Block Diagram of Fault-Tolerant SSMD

3.2 Dynamic Modelling of SSMD for NMPC

Considering single-phase open-circuit fault occurs in phase *a,* it will get OFF, and the current immediately drops to zero. Now consider the three-phase stator self-inductances be L_a, L_b and L_c to L and three-phase stator mutual-inductances be M_{ab}, M_{bc} and M_{ca} to M. Stator phase currents i_b and i_c[44]

$\lambda_{sa}, \lambda_{sb}, \lambda_{sc}$ be the stator flux linkages produced by the stator currents are as shown:

$$\begin{bmatrix} \lambda_{sa} \\ \lambda_{sb} \\ \lambda_{sc} \end{bmatrix} = \begin{bmatrix} M & M \\ L & M \\ M & L \end{bmatrix} \begin{bmatrix} i_b \\ i_c \end{bmatrix} \tag{1}$$

The stator flux linkage vector equation in *abc* frame:

$$\begin{bmatrix} \lambda_a \\ \lambda_b \\ \lambda_c \end{bmatrix} = \begin{bmatrix} \lambda_{sa} \\ \lambda_{sb} \\ \lambda_{sc} \end{bmatrix} \begin{bmatrix} \lambda_m \cos\theta_e \\ \lambda_m \cos(\theta_e - 120°) \\ \lambda_m \cos(\theta_e + 120°) \end{bmatrix} \tag{2}$$

The resultant of stator flux linkages produced by stator currents and rotor magnetic fields along *a, b,* and *c* axes are λ_a, λ_b and λ_c respectively. The electrical rotor angle position is θ_e and the permanent magnet flux linkage is λ_m. At the instant of phase *a* being OFF, the triac gets turned ON. The stator phase voltages vector of PMSM given by:

$$\begin{bmatrix} v_{bn} \\ v_{cn} \end{bmatrix} = \begin{bmatrix} R_b & 0 \\ 0 & R_c \end{bmatrix} \begin{bmatrix} i_b \\ i_c \end{bmatrix} + \frac{d}{dt} \begin{bmatrix} \lambda_b \\ \lambda_c \end{bmatrix} \tag{3}$$

$$\begin{bmatrix} v_{bn} \\ v_{cn} \end{bmatrix} = \begin{bmatrix} R_b & 0 \\ 0 & R_c \end{bmatrix} \begin{bmatrix} i_b \\ i_c \end{bmatrix} + \begin{bmatrix} L & M \\ M & L \end{bmatrix} \begin{bmatrix} \frac{di_b}{dt} \\ \frac{di_c}{dt} \end{bmatrix} - \begin{bmatrix} \lambda_m \omega_r \sin(\theta_e - 120°) \\ \lambda_m \omega_r \sin(\theta_e + 120°) \end{bmatrix} \tag{4}$$

ω_r ------the speed of the rotor.

Here it is assumed that mutual inductance is one half of the phase inductance *L*.

$L_d = L_q = L + M = L + (1/2) L = (2/3) L \tag{5}$

Let us consider the moment of inertia, electromagnetic torque, load torque, coefficient of damping friction be *J,* T_e, T_l *and* B_m respectively.

The electromagnetic torque equation is given by

$$J\frac{d\omega_r}{dt} = T_e - T_l - B_m\omega_r - T_s \tag{6}$$

3.2.1 Proposed NMPC for PMSM Drive for Normal Operating Condition (Pre-Fault) [44]

The state-space(discrete-time) model of the PMSM drive before the occurrence of fault (pre- fault) is given by

$i_{dp}(k + 1) = \Delta i_{d0}(k) + \Delta i_{dp}(k) + i_d(k) \tag{7}$

$i_{qp}(k + 1) = \Delta i_{q0}(k) + \Delta i_{qp}(k) + i_q(k) \tag{8}$

i_{dp} and i_{qp} ------ pre-fault d-axis and q-axis currents, respectively.

$\Delta i_{d0}(k) = [L_s \omega_r(k)i_q(k) - R_s i_d(k)]T_s/L_s$

$\Delta i_{dp}(k) = [v_{dp}(k)]T_s/L_s$

$\Delta i_{q0}(k) = -[L_s \omega_r(k)i_d(k) + R_s i_q(k)]T_s/L_s$

$\Delta i_{qp}(k) = [v_{qp}(k)]T_s/L_s$

$[v_{dp}(k) \quad v_{qp}(k)]^T = P_{3/2} v_{dc}(k)[\omega_{a1}(k) \quad \omega_{b1}(k) \quad \omega_{c1}(k)]^T \tag{9}$

where $P_{3/2}$ is a Park's transformation matrix

$\omega_{a1} = S_a$, $\omega_{b1} = S_b$, $\omega_{c1} = S_c$ ------ the virtual space vectors which are used to calculate d-axis and q-axis voltages by Park's transformation matrix.

The cost function C_p of NMPC for pre-fault must be chosen so that both torque and flux is as close as of reference value:

$$C_p(k+1) = [i_d^r(k+1) - i_{dp}(k+1)]^2 + [i_q^r(k+1) - i_{qp}(k+1)]^2 \tag{10}$$

The minimum value of cost function is defined as

$$\text{Min } C_p = |T_e^r - T_e(k+1)| + k_1||\lambda_s^r| - |\lambda_s(k+1)||$$

$$\text{s.t. } V_s(k) \in \{V_1, V_2, \text{----}, V_6\} \tag{11}$$

T_e^r and λ_s^r ------ torque and stator flux reference values.

$T_e(k+1)$ and $\lambda_s(k+1)$ ------ predictions for torque and stator flux at $(k+1)$th instant, respectively.

$V_1, V_2, \text{----}, V_6$ ------ non zero voltage space vectors generated by a three-phase inverter before the fault.

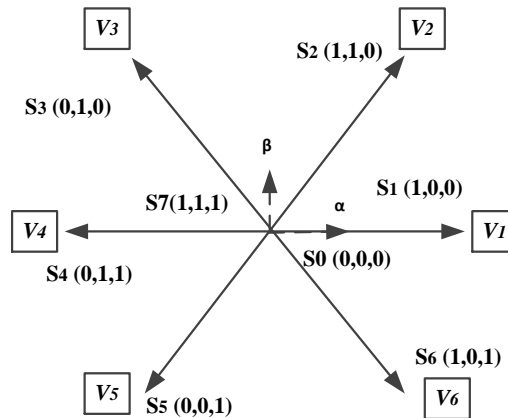Voltage vectors and the corresponding switching states of the inverter is as shown in Figure 6.

Figure 6. Voltage vectors and corresponding switching states of the inverter [4]

3.2.2 Proposed NMPC for PMSM Drive for Faulty Condition (Post-Fault)

      The discrete-time state-space model of the faulty PMSM drive is given by

$$i_{df}(k+1) = \Delta i_{d0}(k) + \Delta i_{df}(k) + i_d(k) \tag{12}$$

$$i_{qf}(k+1) = \Delta i_{q0}(k) + \Delta i_{qf}(k) + i_q(k) \tag{13}$$

i_{df} and i_{qf} ------ post fault d-axis and q-axis currents, respectively.

Let v_{df} and v_{qf} be the d-axis and q-axis voltages:

$$\Delta i_{df}(k) = [v_{df}(k)]T_s/L_s$$

$$\Delta i_{qf}(k) = [v_{qf}(k)]T_s/L_s$$

The cost function C_f of NMPC for the post-fault is given by

$$C_f(k+1) = [i_d^r(k+1) - i_{df}(k+1)]^2 + [i_q^r(k+1) - i_{qf}(k+1)]^2 \tag{14}$$

In the NMPC algorithm, while evaluating cost function, the stator phase voltages (Vbn and Vcn) are directly employed instead of voltage space vector.

The minimum cost function value is

$$\text{Min } C_f = |T_e^r - T_e(k+1)| + k_1||\lambda_s^r| - |\lambda_s(k+1)||$$

$$\text{s.t. } V_{sn}(k+1) \in \{V_{bn1\_cn1}, V_{bn2\_cn2}, \text{.......} V_{bn6\_cn6}\} \} \tag{15}$$

where V_{bni_cni} (i=1, 2, ….,6) represents two stator phase voltages V_{bn} and V_{cn6}.

In NMPC, the phase currents predicted in abc reference frame instead of d-q. Therefore equation (4) can be rewritten as

$$\frac{di_b}{dt} = \frac{1}{L^2 - M^2}[LV_{bn} - MV_{cn} + MR_c i_c - R_b L i_b + L\lambda_m \omega_r \sin(\theta_e - 120°) - M\lambda_m \omega_r \sin(\theta_e + 120°) \tag{16}$$

$$\frac{di_c}{dt} = \frac{1}{L^2 - M^2}[LV_{cn} - MV_{bn} + MR_b i_b - LR_c i_c + L\lambda_m \omega_r \sin(\theta_e + 120°) - M\lambda_m \omega_r \sin(\theta_e - 120°) \tag{17}$$

      The prediction of stator current at next sampling instant based on given stator voltages $V_{bn}(k), V_{cn}(k)$ and measured currents $i_b(k), i_c(k)$ at the current sampling instant.

$i_b(k + 1) = i_b(k) + \frac{Ts}{L^2 - M^2}[LV_{bn}(k) - MV_{cn}(k) + MR_ci_c(k) - R_bLi_b(k)$

$+L\lambda_m(k) \; \omega_r(k) \sin(\theta_e(k) - 120°) - M\lambda_m(k) \; \omega_r \sin(\theta_e(k) + 120°)$

(18)

$i_c(k + 1) = i_c(k) + \frac{Ts}{L^2 - M^2}[LV_{cn}(k) - MV_{bn}(k) + MR_bi_b(k) - R_cLi_c(k)$

$+L\lambda_m(k) \; \omega_r(k) \sin(\theta_e(k) + 120°) - M\lambda_m(k) \; \omega_r \sin(\theta_e(k) - 120°)$

(19)

where $i_b(k + 1)$ and $i_c(k + 1)$ are predicted values for the stator currents for the next sampling period, Ts.
After getting $i_b(k + 1)$ and $i_c(k + 1)$ both the torque and flux at the $(k + 1)$th instant can be estimated.

3.2.3 Torque Estimation

The electromagnetic torque equation is given by

$T_e(k + 1) = \frac{3}{2}p[\lambda_m(k + 1)i_q(k + 1) + (L_d - L_q)i_d(k + 1) \; i_q(k + 1)]$ (20)

p is the number of pole pairs.

3.2.4 Flux Estimation

Flux linkage expression can be given by

$\begin{bmatrix} \lambda_d(k + 1) \\ \lambda_q(k + 1) \end{bmatrix} = \begin{bmatrix} L_d & 0 \\ 0 & L_q \end{bmatrix} \begin{bmatrix} i_d(k + 1) \\ i_q(k + 1) \end{bmatrix} + \begin{bmatrix} \lambda_m(k + 1) \\ 0 \end{bmatrix}$ (21)

L_d, L_q and i_d, i_q ------ d-q system inductances and currents, respectively.

Using Park and Clarke transformations, $i_d \; and \; i_q$ can be calculated as

$\begin{bmatrix} i_d(k + 1) \\ i_q(k + 1) \end{bmatrix} = \begin{bmatrix} \cos\theta_e(k + 1) & -\sin\theta_e(k + 1) \\ \sin\theta_e(k + 1) & \cos\theta_e(k + 1) \end{bmatrix} \begin{bmatrix} -1/2 & -1/2 \\ \sqrt{3}/2 & -\sqrt{3}/2 \end{bmatrix} \begin{bmatrix} i_b(k + 1) \\ i_c(k + 1) \end{bmatrix}$ (22)

Finally, the stator flux linkage is given by

$\lambda_s(k + 1) = \sqrt{[\lambda_d(k + 1)]^2 + [\lambda_q(k + 1)]^2}$ (23)

The desired reference stator flux linkage obtained by maximum torque per ampere algorithm

$\lambda_s^r = \sqrt{\left[T_e^r L_q \lambda_d / \frac{3}{2}p \; \lambda_m\right]^2 + [i_d^r L_d + \lambda_m]^2}$ (24)

Where i_d^r is assumed to be zero

Hence, $\lambda_s^r = \sqrt{\left[T_e^r L_q \lambda_d / \frac{3}{2}p \; \lambda_m\right]^2 + \lambda_m^2}$ (25)

4. ANALYSIS OF SSMD FOR NMPC

Analysis of SSMD for NMPC carried out using the LUCAS NULLE servo drive system.
4.1 Specification of synchronous servo motor used for the analysis of proposed NMPC
Table 1 shows the parameters of the synchronous servo motor for the proposed NMPC.

Table1. Parameters of Synchronous Servo Motor [50]

Parameter	Symbol	Value
Armature resistance	R_s	4.74Ω
Armature inductance	L_s	8.6 e^{-3} H
Moment of Inertia	J	0.33 Kg.cm^2
Permanent-magnet flux	λ_m	0.089Wb
Number of poles	P	8
Standstill current	I_o	2.99 A
Peak current	I_{omax}	12 A
Reference Speed	ω_r	1000 rpm

4.2 Experimental Set-up

Figure 7 shows the experimental set-up of the Lucas Nulle servo drive system for NMPC. It comprises a self-commutated converter, MATLAB interface for power electronics, three-phase isolating transformer 300 VA, synchronous servo motor 0.3 kW, and incremental position encoder with 1024 pulses analog/digital multimeter, wattmeter and power factor meter, servo test stand for 0.3 kW machines.
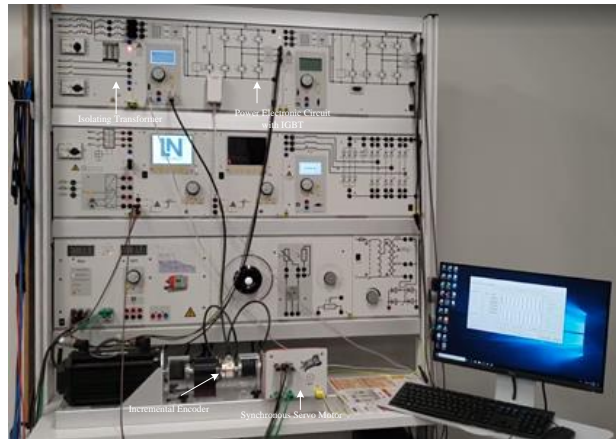

Figure 7. Experimental set-up of SSMD for NMPC

4.3 Results

Figures 8 and 9 show the simulation and experimental results for three-phase currents for SSMD employing NMPC before the fault.
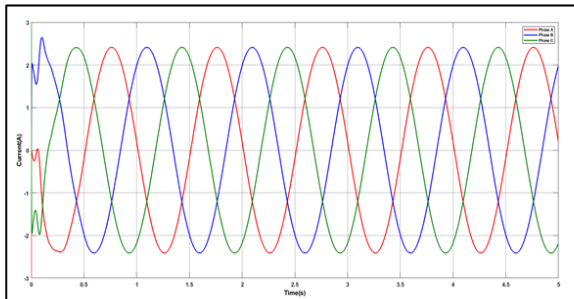

Figure 8. Simulation result of Three-Phase Currents
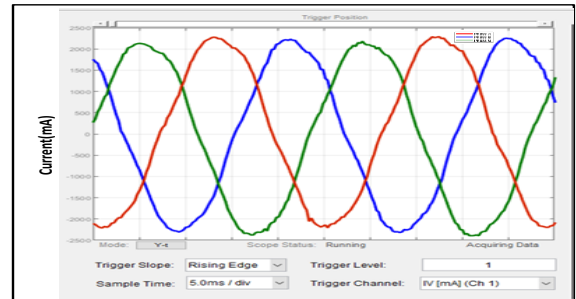

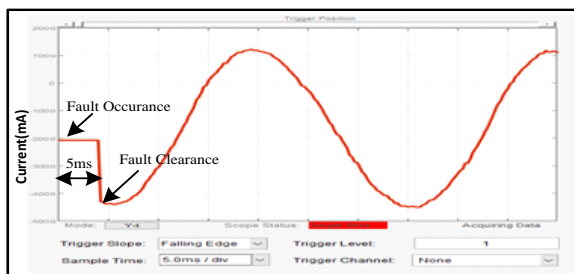Figure 9. Experimental result of Three-Phase Currents

Figure 10. Phase A current under SOCF fault
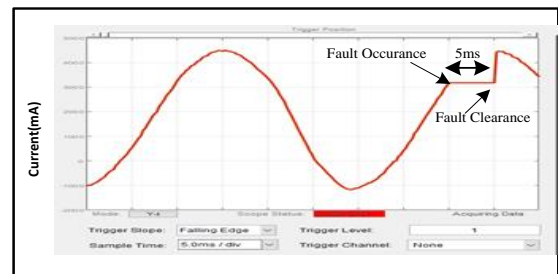(Speed=500 rpm)

Figure 11. Phase A current under SOCF fault
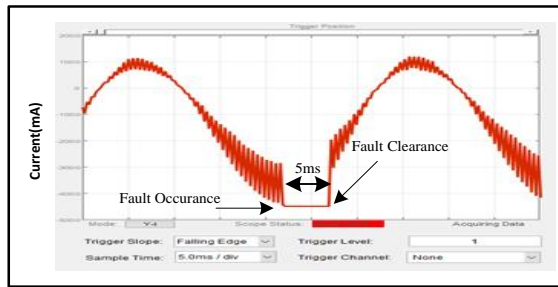(Speed=1000 rpm)

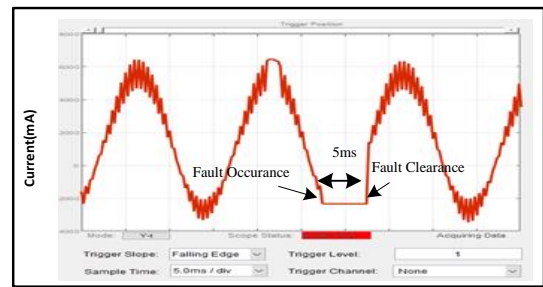Figure 12. Phase A current under SCF fault
(Speed=500 rpm)

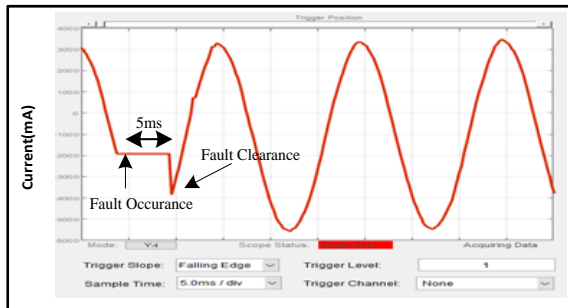Figure 13. Phase A current under SCF fault
(Speed=1000 rpm)

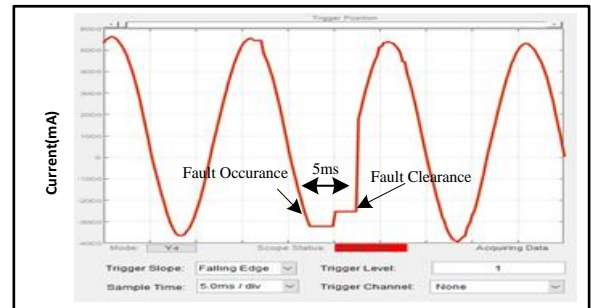Figure 14. Phase A current under DF fault
(Speed=500 rpm)

Figure 15. Phase A current under DF fault
(Speed=1000 rpm)

Figure 10 – Figure 15 shows that employing novel model predictive control, the fault clearance time for all the three different types of faults that occurred in servo drive is short, which is less than 5 ms compared to the other fault-tolerant algorithms.

5. CONCLUSION

In this paper, a fault-tolerant synchronous servo motor drive (SSMD) considering a real-time fault diagnostic method employing novel model predictive control has been presented. Here the three different types of faults; single-phase open-circuit fault (SOCF), short circuit fault (SCF), and permanent magnet demagnetization fault (DF) under parameter mismatch of a PMSM drive are considered. Implementation of the proposed algorithm for SSMD, employing novel model predictive control considering circuit faults performed using Lucas Nulle Servo Drive system with MATLAB Simulink. The experimental results show the effectiveness of the proposed algorithm.

REFERENCES

[1]   Jan A. Melkebeek, *Electrical Machines and Drives: Fundamentals and Advanced Modelling* , Springer, 2018.

[2]   W.H.Ali, S.A.Abood, M.N.O.Sadiku, *Fundamentals of Electrical Machines: A Primer with MATLAB*, Boca Raton, FL, USA: CRC Press, 2019.

[3]   Austin Hughes and Bill Drury, *Electric Motors and Drives: Fundamentals, Types, and Application*, Elsevier, 2019.

[4]   I. Jlassi, J.Estima, S.K.Khill, and N.B, Bellaaj, "A Robust Observer-Based Method for IGBTs and Current Sensors Fault Diagnosis in Voltage-Source Inverters of PMSM Drives," *IEEE Trans. Ind. Appl*., vol. 53, no. 3, pp. 2894–2905, May/June 2017.

[5]   B.Vaseghi, B.N.Mobarakeh, N.Tacorabet, and F.M.Tabar, "Inductance Identification and Study of PM Motor with Winding Turn Short Circuit Fault," *IEEE Trans. Magnetics*., vol. 47, no. 5, pp. 978–981, May 2011.

[6]   T.Boileau, N.Leboeuf, B.N.Mobarakeh and F.M.Tabar, "Synchronous Demodulation of Control Voltages for Stator Interturn Fault Detection in PMSM," *IEEE Trans. Power Electron*., vol. 28, no.12, pp. 5647–5654, Dec.2013.

[7]   R.Z.Haddad, C.A.Lopez, S.N. Foster, and E.G.Strangas, "A Voltage-Based Approach for Fault Detection and Separation in Permanent Magnet Synchronous Machines," *IEEE Trans. Ind. Appl*., vol.53, no.6, pp. 5305–5314, Nov/Dec 2017.

[8]   L. Cheng, Y.Sui, P.Zheng, and F.Wu "Implementation of Postfault Decoupling Vector Control and Mitigation of Current Ripple for Five-Phase Fault-Tolerant PM Machine Under Single-Phase Open-Circuit Fault," *IEEE Trans. Power Electron*., vol. 33, no.10, pp. 8623–8635, Oct.2018.

[9]   J. Rodriguez, R.M.Kennel, J.R.Espinoza, M.Trincado, C.A.silva, and C.A.Rozas, "High-performance control strategies for electrical drives: An experimental assessment," *IEEE Trans. Ind. Electron.*, vol. 59, no. 2, pp. 812–820, Feb. 2012.

[10]   H. A. Young, M.A.Perez, and J.Rodriguez, "Analysis of finite-control set model predictive current control with model parameter mismatch in a three-phase inverter," *IEEE Trans. Ind. Electron.*, vol. 63, no. 5, pp. 3100–3107, Jan. 2016.

[11]   W. Xie, X.Wang, W. Xu, R.M.Kennel, "Finite-Control-Set Model Predictive Torque Control with a Deadbeat Solution for PMSM Drive ," *IEEE Trans. Ind. Electron.*, vol. 62, no. 9, pp. 5402–5410, Sep. 2015.

[12]   T.Tarczewski and L. M. Grzesiak, "Constrained State Feedback Speed Control of PMSM Based on Model Predictive Approach," *IEEE Trans. Ind. Electron.*, vol. 63, no. 6, pp. 3867–3875, June 2016.

[13]   E. Fuentes, C. A. Silva and R. M. Kennel, "MPC Implementation of a Quasi-Time-Optimal Speed Control for a PMSM Drive, With Inner Modulated-FS-MPC Torque Control," *IEEE Trans. Ind. Electron.*, vol. 63, no. 6, pp. 3897-3905, June 2016, doi: 10.1109/TIE.2016.2519326.

[14]   T. Türker, U. Buyukkeles, and A. F. Bakan, "A Robust Predictive Current Controller for PMSM Drives," *IEEE Trans. Ind. Electron.*, vol. 63, no. 6, pp. 3906–3914, June 2016.

[15]   Z. Mynar, L. Vesely, and P.Vaclavek, "PMSM Model Predictive Control with Field-Weakening Implementation," *IEEE Trans. Ind. Electron.*, vol. 63, no. 8, pp. 5156–5166, Aug. 2016.

[16]   M. Yang, X. Lang, J. Long, and D. Xu, " Flux Immunity Robust Predictive Current Control With Incremental Model and Extended State Observer for PMSM Drive," *IEEE Trans. Ind. Electron.*, vol. 32, no. 12, pp. 9267–9279, Dec. 2017.

[17]   Z. Zhou, C. Xia, Y. Yan, Z. Wang, and T. Shi, "Torque Ripple Minimization of Predictive Torque Control for PMSM With Extended Control Set," *IEEE Trans. Ind. Electron.*, vol. 64, no. 9, pp. 6930–6939, Sep. 2017.

[18]   A. Dey, P.P.Rajeevan, R.Ramchand, K. Matthew, and K.Gopakumar, "A space-vector-based hysteresis current controller for a general n-level inverter-fed drive with nearly constant switching frequency control," *IEEE Trans. Ind. Electron.*, vol. 60, no. 5, pp. 1989–1998, May 2013.

[19]   J.W. Jung, V.Q.Liu, T.D.Do, E.K.Kim, and H.H.Choi, "Adaptive PID speed control design for permanent magnet synchronous motor drives," *IEEE Trans. Power Electron.*, vol. 32, no. 2, pp. 900–908, Mar. 2015.

[20]   S. C. Carpiuc and C. Lazar, "Fast real-time constrained predictive current control in permanent magnet synchronous machine-based automotive traction drives," *IEEE Trans. Transport. Electrific.*, vol. 1, no. 4, pp. 326–335, Oct. 2015.

[21]   R. Cai, R.Zheng, M.Liu, and M.Li, "Robust Control of PMSM Using Geometric Model Reduction and μ-Synthesis," *IEEE Trans. Ind. Electron.*, vol. 65, no. 1, pp. 498–509, Jan. 2018.

[22]   W.H.Ali, M.Gowda, P.Cofie, and J. Fuller, " Design of a speed controller using extended kalman filter for PMSM," *in Proc. of IEEE 57th International Midwest Symposium on Circuits and Systems (MWSCAS)*, Aug.2014, pp. 1101–1104.

[23]   W.Wang, J.Zhang, and M. Cheng, " Common model predictive control for permanent-magnet synchronous machine drives considering single-phase open-circuit fault," *IEEE Trans. Power Electron.*, vol. 32, no. 7, pp. 5862–5872, July 2017.

[24]   R. Sultana and S. K. Sahoo, "Finite control set model predictive current control for a cascaded multilevel inverter," *J. Electr .Eng. Technol.*, vol. 11, no. 6, pp. 1674–1683, Nov. 2016.

[25]   M. P. Akter, "Model predictive control of bidirectional AC-DC converter for energy storage system," *J. Electr .Eng. Technol.,* vol. 10, no.1, pp. 165–175, Jan. 2015.

[26]   Z. Song, Y. Tian, W. Chen, Z. Zou, and Z. Chen, "Predictive duty cycle control of three-phase active-front-end rectifiers," *IEEE Trans. Power Electron.*, vol. 31, no. 1, pp. 698–710, Jan. 2016.

[27]   S. Mariethoz and M. Morari, "Explicit model-predictive control of a pwm inverter with an LCL filter," *IEEE Trans. Ind. Electron.*, vol. 56, no. 2, pp. 389-399, Feb. 2009.

[28]   R. Baidya, R. P. Aguilera, P. Acuna, R. Delgado, T. Geyer, D. Quevedo, and T. Mouton, "Fast multistep finite control set model predictive control for transient operation of power converters," *Proc. IEEE Ind. Electron. Conf.*, Florence, Italy, pp. 5039–5045, Oct. 2016.

[29]   S. Vazquez, J. I. Leon, L. G. Franquelo, J. Rodriguez, H. A. Young, A. Marquez, and P. Zanchetta, "Model predictive control: A review of its applications in power electronics," *IEEE Ind. Electron. Mag.*, vol. 8, no. 1, pp. 16–31, Mar. 2014.

[30]   A. Bemporad, M. Morari, V. Dua, and E. Pistikopoulos, "The explicit linear quadratic regulator for constrained systems," *Automatica*, vol. 38, no. 1, pp. 3–20, 2002.

[31]   A. Bemporad, F. Borrelli, and M. Morari, "Model predictive control based on linear programming, the explicit solution," *IEEE Trans. Autom. Contr.*, vol. 47, no. 12, pp. 1974–1985, 2002.

[32]   S. Mariethoz and M. Morari, "Explicit model predictive control of a PWM inverter with an LCL filter," *IEEE Trans. Ind. Electron.*, vol. 56, pp. 389–399, Feb. 2009.

[33]   S. Richter, S. Mariethoz, and M. Morari, "Highspeed online MPC based on a fast gradient method applied to power converter control," in *Proc. American Control Conf. (ACC),* 2010, pp. 4737–4743.

[34]   J. Neely, S. Pekarek, R. DeCarlo, and N. Vaks, "Real-time hybrid model predictive control of a boost converter with constant power load," in *Proc. 25th Annu. IEEE Applied Power   Electronics Conf. Exposition (APEC)*, Feb. 2010, pp. 480–490.

[35]   H. Mahmoudi, M. Aleenejad, and R. Ahmadi, " Modulated Model Predictive Control for a Z-Source-Based Permanent Magnet Synchronous Motor Drive System," *IEEE Trans. Power Electron.*, vol. 65, no.10, pp. 8307–8318, Oct. 2018.

[36]   P. Brandstetter, M. Kuchar, H. H. Vo and C. S. Thien Dong, "Induction motor drive with PWM direct torque control," *2017 18th International Scientific Conference on Electric Power Engineering (EPE)*, Kouty nad Desnou, 2017, pp. 1-5.

[37]   Gourikrishna and V. R. Bindu, "PWM Direct Torque Control of Induction Motor Drive with Reduced Torque Ripple," *2018 International CET Conference on Control, Communication, and Computing (IC4)*, Thiruvananthapuram, 2018, pp. 33-38.

[38]   Y. Zhang and C. Qu, "Direct Power Control of a Pulse Width Modulation Rectifier Using Space Vector Modulation Under Unbalanced Grid Voltages," *IEEE Trans. on Power Electron.*, vol. 30, no. 10, pp. 5892-5901, Oct. 2015.

[39]   Z. Wang, J. Chen, M. Cheng and K. T. Chau, "Field-Oriented Control and Direct Torque Control for Paralleled VSIs Fed PMSM Drives With Variable Switching Frequencies," *IEEE Trans. on Power Electron.*, vol. 31, no. 3, pp. 2417-2428, March 2016.

[40]   M. H. Zamani, G. H. Riahy and M. Abedi, "Rotor-Speed Stability Improvement of Dual Stator-Winding Induction Generator-Based Wind Farms By Control-Windings Voltage Oriented Control," *IEEE Trans. on Power Electron.*, vol. 31, no. 8, pp. 5538-5546, Aug. 2016.

[41]   J. Lee and K. Lee, "Carrier-Based Discontinuous PWM Method for Vienna Rectifiers," *IEEE Trans. on Power Electron.*, vol. 30, no. 6, pp. 2896-2900, June 2015.

[42]   R. S. Kaarthik, K. Gopakumar, C. Cecati and I. Nagy, "Timing Calculations for a General N-Level Dodecagonal Space Vector Structure Using Only Reference Phase Voltages," *IEEE Trans. Ind. Electron.*, vol. 63, no. 3, pp. 1395-1403, March 2016.

[43]   J. Meili, S. Ponnaluri, L. Serpa, P. K. Steimer and J. W. Kolar, "Optimized Pulse Patterns for the 5-Level ANPC Converter for High Speed High Power Applications," *IECON 2006 - 32nd Annual Conference on IEEE Industrial Electronics*, Paris, 2006, pp. 2587-2592.

[44]   W. H. Ali, Y.P. Akhare, P. Cofie, J. H. Fuller, J. Attia, "Novel Fault Tolerant Predictive Control for Analysis of Open Circuit Fault in a PMSM Drive," *American Journal of Engineering Research (AJER)*, vol.8, no.06, 2019, pp.177-183

[45]   Tobias Geyer, Model Predictive Control of High Power Converters and industrial drives Wiley,2016.

[46]   M. Bacic, M. Cannon, Y. I. Lee and B. Kouvaritakis, "General interpolation in MPC and its advantages," *IEEE Transactions on Automatic Control*, vol. 48, no. 6, pp. 1092-1096, June 2003.

[47]   C. Chen, J. Wang, Y. Heo and S. Kishore, " MPC-Based Appliance Scheduling for Residential Building Energy Management Controller," *IEEE Transactions on Smart Grid*, vol. 4, no. 3, pp. 1401-1410, Sept. 2013.

[48]   C. Wang, M. Yang, W. Zheng, J. Long and D. Xu, " Vibration Suppression With Shaft Torque Limitation Using Explicit MPC-PI Switching Control in Elastic Drive Systems," *IEEE Trans. on Ind. Electron.*, vol. 62, no. 11, pp. 6855-6867, Nov. 2015.

[49]   S. S. Yeoh, T. Yang, L. Tarisciotti, C. I. Hill, S. Bozhko, and P. Zanchetta, "Permanent-Magnet Machine-Based Starter–Generator System With Modulated Model Predictive Control," *IEEE Transactions on Transportation Electrification*, vol. 3, no. 4, pp. 878-890, Dec. 2017.

[50]   Department of Electrical Engineering, "Lab Manual for servo machine testing stand," Roy G. Perry College of Engineering, Prairie View A & M University, Prairie View, Texas, USA.

AUTHORS DETAILS

Yogita P. Akhare received her Bachelor of Engineering (B.E.) in Electronics & Power (Electrical) from Nagpur University, Nagpur, Maharashtra, India, and Master of Engineering (M.E.) in Electrical (Power Systems) from Pune University, Maharashtra, India. She is currently working towards a Ph.D. degree in Electrical Engineering at Prairie View A&M University, Prairie View, Texas.Her current research interests include Electrical Machine Drives and Nanotechnology.

Dr. Warsame H. Ali received his B. Sc. from King Saud University, Electrical Engineering Department, Riyadh, Saudi Arabia, and his M.Sc. from Prairie View A&M University, Prairie View, Texas. He received his Ph.D. in Electrical Engineering from the University of Houston, Houston, Texas. Dr. Ali was promoted to Associate Professor and tenure in 2010 and Full Professor in 2017. Dr. Ali joined NASA, Glenn Research Center in the summer of 2005, and Texas Instruments (TI) in 2006. Dr. Ali has given several invited talks and is also the author of 80 research articles in major scientific journals and conferences. Dr. Ali has received several major NSF, NAVSEA, AFRL, and DOE awards. He published two textbooks titled "Signals and Systems: A Primer with MATLAB" and "Fundamentals of Electric Machine: A Primer with MATLAB". He is currently teaching

undergraduate and graduate courses in the Electrical and Computer Engineering department at Prairie View A&M University. His main research interests are the Application of Digital PID Controllers, Digital Methods to Electrical   Measurements, Mixed Signals Testing Techniques, Power Systems, HVDC Power Transmission, Sustainable Power and Energy Systems, and Power Electronics and Motor drives, Electric and Hybrid Vehicles, Smart Grid and Multivariable Control Systems. Moreover, Dr. Ali is a registered Professional Engineer in the State of Texas.

Dr. John Fuller is a Professor of Electrical and Computer Engineering at Prairie View A&M University in Prairie View, Texas. He received a BSEE degree from Prairie View A&M University and a master's and Ph.D. degree from the University of Missouri-Columbia. He has conducted research on several funded projects over his thirty-nine-year teaching career in Higher Education with notable accomplishments of a PVAMU solar-powered car and research in nuclear characterization and Nuclear Sensors/Detectors. He has been recognized for his accomplishments at the University with numerous awards for teaching, research, and service. He is a registered Professional Engineer in the State of Texas in addition to teaching and research duties. He has also held administrative positions of Department Head of Electrical Engineering and Interim Dean of the College of Engineering at Prairie View A&M University.

Dr. John Okyere Attia is a Professor of Electrical and Computer Engineering at Prairie View A&M University. He was the Department Head of the Electrical and Computer Engineering Department from 1997 to 2013.   He also served as Interim Associate Dean. Dr. Attia has worked on projects funded by the National Science Foundation, NASA, Texas Higher Education Coordinating Board, and the Texas Workforce Commission. Dr. Attia has more than 80 technical publications. He has published in refereed journal papers and refereed conference papers and the author of five books published by the CRC Press. He has supervised to completion of several Ph.D. dissertations and MS thesis work of students. Moreover, Dr. Attia is a registered Professional Engineer in the State of Texas.

.